Received 31 August 2015
Revised 9 October 2015
Accepted 30 October 2015

Numerical investigation of CuO-water nanofluid turbulent convective heat transfer in square cross-section duct under constant heat flux

Hsien-Hung Ting and Shuhn-Shyurng Hou
Department of Mechanical Engineering,
Kun Shan University, Tainan, Taiwan

Abstract

Purpose – The purpose of this paper is to numerically investigate the convective heat transfer of water-based CuO nanofluids flowing through a square cross-section duct under constant heat flux in the turbulent flow regime.

Design/methodology/approach – The numerical simulation is carried out at various Peclet numbers and particle concentrations (0.1, 0.2, 0.5, and 0.8 vol%). The finite volume formulation is used with the semi-implicit method for pressure-linked equations algorithm to solve the discretized equations derived from the partial nonlinear differential equations of the mathematical model.

Findings – The heat transfer coefficients and Nusselt numbers of CuO-water nanofluids increase with increases in the Peclet number as well as particle volume concentration. Also, enhancement of the heat transfer coefficient is much greater than that of the effective thermal conductivity at the same nanoparticle concentration.

Research limitations/implications – Simulation of nanofluids turbulent forced convection at very high Reynolds number is worth for further study.

Practical implications – The heat transfer rates through non-circular ducts are smaller than the circular tubes. Nevertheless, the pressure drop of the non-circular duct is less than that of the circular tube. This study clearly presents that the nanoparticles suspended in water enhance the convective heat transfer coefficient, despite low volume fraction between 0.1 and 0.8 percent. Adding nanoparticles to conventional fluids may enhance heat transfer performance through the non-circular ducts, leading to extensive practical applications in industries for the non-circular ducts.

Originality/value – Few papers have numerically studied convective heat transfer properties of nanofluids through non-circular ducts. The present numerical results show a good agreement with the published experimental data.

Keywords Convective heat transfer, Nanofluid, Square cross-section duct, Turbulent flow

Paper type Research paper

Nomenclature

A	surface area of square cross-section duct (m^2)	G	generation of turbulent kinetic energy
C	specific heat ($J\,kg^{-1}\,K^{-1}$)	$\overline{h_{nf}}$(exp)	experimental average nanofluid heat transfer coefficient ($W\,m^{-2}\,K^{-1}$)
D_h	hydraulic diameter (m)		

Conflict of interest: the authors declare that there is no conflict of interest regarding the publication of this paper.

This work was supported by the Ministry of Science and Technology, Taiwan, under contract of MOST 103-2221-E-168-013.

Engineering Computations: International Journal for Computer-Aided Engineering and Software
Vol. 33 No. 6, 2016
pp. 1714-1728

0264-4401
DOI 10.1108/EC-08-2015-0261

$\overline{h_{nf}}(sim)$	simulated average nanofluid heat transfer coefficient ($W m^{-2} K^{-1}$)
$\overline{h_{nf}}(th)$	theoretical average nanofluid heat transfer coefficient ($W m^{-2} K^{-1}$)
k	thermal conductivity ($W m^{-1} K^{-1}$)
L	duct length (m)
$\overline{Nu}$(exp)	experimental average nanofluid Nussult number
$\overline{Nu}(th)$	theoretical average nanofluid Nusselt number calculated from Dittus-Boelter equation
$\overline{P}$	time-averaged pressure (Pa)
Pe	Peclet number
Pr	Prandtl number
q	heat flux (W)
Re	Reynolds number
T	temperature (K)
$\overline{T}$	time-averaged mean temperature (K)
$\overline{t'}$	fluctuations in temperature (K)
$\overline{U}$	average fluid velocity at inlet ($m s^{-1}$)
$\overline{u'}$	fluctuations in velocity ($m s^{-1}$)
$\overline{V}$	time-averaged mean velocity ($m s^{-1}$)

Greek symbols

γ	ratio of nano-layer thickness to original particle radius
ε	rate of dissipation ($J kg^{-1} s^{-1}$)
κ	turbulent kinetic energy ($J kg^{-1}$)
μ	viscosity (Pa s)
ρ	density ($kg m^{-3}$)
σ	effective Prandtl number
ϕ	nanoparticle volume fraction (percent)

Subscripts

nf	nanofluid
b	bulk
bf	base fluid
i	inlet
w	water or wall
o	outlet
κ	refers to turbulent kinetic energy
ε	refers to rate of dissipation

1. Introduction

Nanofluids are a new class of heat transfer fluids. Typically, nanofluids contain nanoparticles with sizes of 1 to 100 nm dispersed in a conventional liquid (base fluid) such as water, ethylene glycol, or engine oil. The thermal conductivities of nanofluids with suspended metallic or nonmetallic particles are expected to be much higher than those of conventional heat transfer fluids. As a result, the suspended nanoparticles can significantly change the transport and thermal properties of the base fluid. Considerable enhancement of forced convective heat transfer has been widely reported for Al_2O_3-water (Bianco *et al.*, 2013, 2014), Cu-water (Sheikholeslami *et al.*, 2014b; Ellahi *et al.*, 2015), CuO-water (Akbar *et al.*, 2014; Sheikholeslami *et al.*, 2014a), and TiO_2-water-based (Akbar *et al.*, 2014) experimental systems.

Eastman *et al.* (1999) studied the enhancement of the thermal conductivity of CuO-water nanofluid compared to that of the base fluid. They found an approximately 20 percent enhancement of effective thermal conductivity when 5 vol% CuO nanoparticles were added to water. In addition, compared with the base fluid, an improvement of higher than 15 percent in the heat transfer coefficient was observed when 0.9 vol% particles were added to the base fluid under the turbulent flow condition.

Xuan and Li (2003) conducted an experimental study and found an increase of up to 28 percent in the convective heat transfer coefficient for the turbulent flow regime of CuO-water nanofluid in a tube when the Reynolds number ranged from 10,000 to 25,000.

Mirmasoumi and Behzadmehr (2008) numerically investigated the effect of nanoparticle diameter on the convective heat transfer performance of Al_2O_3-water nanofluid flowing under a fully developed laminar flow regime. They found that decreasing the nanoparticle diameter significantly increased the heat transfer coefficient of the nanofluid; the nanoparticle diameter had no significant effect on the skin friction coefficient.

Shahi *et al.* (2010) numerically studied the laminar convective heat transfer of CuO-water nanofluid flowing through a square cavity under a laminar flow regime. They reported that with increasing particle concentration, the average Nusselt number of the nanofluid increased, but the bulk temperature of the nanofluid decreased.

Mohammed *et al.* (2011a, b) numerically investigated the effect of four nanofluids (Al_2O_3, SiO_2, Ag, and TiO_2) on the performance of parallel square and rectangular microchannel heat exchangers. Their results showed that with an increase in the Reynolds number, the heat transfer coefficient of the nanofluid increased, whereas the average bulk temperature of the cold fluid decreased.

Etemad *et al.* (2012) investigated the turbulent flow heat transfer performance of Al_2O_3-water and CuO-water nanofluids flowing through a circular channel subjected to a constant temperature. They reported relative enhancements in the Nusselt number of 1.29 and 1.30 for the nanofluids at a Peclet number of 55,000 with 2 vol% γ-Al_2O_3 and CuO nanoparticles, respectively.

In a recent study, a series of cracking reactions of liquid hydrocarbon-based palladium nanofluids under various cracking conditions were conducted to verify the catalytic ability of the palladium nanoparticles (Yue *et al.*, 2014). The results showed that nanofluids composed of decalin- and kerosene-based nanofluids and palladium nanoparticles had higher performance of heat sink than that of the base fluids under the same cracking conditions.

More recently, Mwesigye and Huan (2015) used the entropy generation minimization method to obtain thermodynamically optimal conditions and geometries for turbulent forced convection of Al_2O_3-water nanofluid in a circular tube. It was found that there is an optimal cross-sectional area at each Reynolds number for which the entropy generation in the tube is a minimum. The optimal cross-sectional area increases as the Reynolds number increases. Ahmed *et al.* (2015) experimentally investigated the effect of nanofluids combined with a vortex generator on the heat transfer and pressure drop characteristics in an equilateral triangular duct. The enhancement of heat transfer was affected by the type of nanofluid and nanoparticle concentration. The maximum augmentations in the Nusselt number obtained were 44.64 and 41.82 percent at 1 vol% and $Re \approx 4{,}000$ for SiO_2-water and Al_2O_3-water nanofluids, respectively.

Many studies have considered the convective heat transfer characteristics of nanofluids using a circular tube under constant wall heat flux. However, few papers have numerically studied the convective heat transfer properties of nanofluids flowing through non-circular ducts. The present study numerically investigates the characteristics of the convective heat transfer of water-based CuO nanofluids flowing through a square cross-section duct with a constant heat flux under turbulent flow conditions. The nanoparticle size is set to 40 nm and four particle concentrations (0.1, 0.2, 0.5, and 0.8 vol%) are considered. Additionally, the effect of the Peclet number on the convective heat transfer coefficient is investigated and the results are compared with those of Mehrjou *et al.*'s study (2015).

2. Mathematical modeling

2.1 Assumptions and governing equations

In this numerical study, the single-phase approach for nanofluids is employed (Koo and Kleinstreuer, 2005; Santra *et al.*, 2009; Ting and Hou, 2015). It is assumed that the base fluid and nanoparticles are perfectly mixed and thus can be treated as a homogeneous mixture. The flow is turbulent. Moreover, it is assumed that the fluid phase and solid particles are in thermal equilibrium and move with the same local velocity considering

the ultra-fine size (40 nm) and low volume fraction (0.8 vol%) of the solid particles. The thermophysical properties of the base fluid (water) and the solid nanoparticles (CuO) used in the present study were adopted from Ho *et al.* (2008) and Heris *et al.* (2011). They are specified in Table I.

The following nonlinear governing equations, namely those for the conservation of mass, momentum, and energy for the nanofluid flow inside the square cross-section duct, represent the mathematical formulation of the single-phase model.

Conservation of mass:

$$div(\rho \overline{V}) = 0 \tag{1}$$

Conservation of momentum:

$$div(\rho \overline{V}\,\overline{V}) = -\nabla \overline{P} + \mu \nabla^2 \overline{V} - div(\rho \overline{u'}\,\overline{u'}) \tag{2}$$

Conservation of energy:

$$div(\rho \overline{V} C_P \overline{T}) = div(k \nabla \overline{T} - \rho C \overline{u'}\,\overline{t'}) \tag{3}$$

where $\overline{V}, \overline{P}$, and $\overline{T}$ are the time-averaged flow variables (i.e. the time-averaged fluid velocity, pressure, and temperature, respectively); ρ, μ, k, and C are the density, dynamic viscosity, thermal conductivity, and specific heat capacity, respectively; and $\overline{u'}$ and $\overline{t'}$ represent the fluctuations in velocity and temperature, respectively. The terms $\rho \overline{u'}\,\overline{u'}$ and $\rho C \overline{u'}\,\overline{t'}$ represent the turbulent shear stress and turbulent heat flux, respectively. These terms are unknown and must be approximately expressed in terms of mean velocity and temperature.

2.2 Physical properties of nanofluid

The physical properties of the nanofluid, namely density, specific heat capacity, thermal conductivity, and viscosity, are defined as follows.

The effective density ρ_{nf} of the nanofluid (Buongiorno, 2006; Corcione, 2010) is:

$$\rho_{nf} = (1-\phi)\rho_{bf} + \phi \rho_p \tag{4}$$

where ρ_{bf} and ρ_P are the mass densities of the base fluid and the nanoparticles, respectively.

The effective specific heat capacity C_{nf} of the nanofluid (Kakaç and Pramuanjaroenkij, 2009; Corcione, 2010) is:

$$C_{nf} = \frac{(1-\phi)(\rho C)_{bf} + \phi (\rho C)_P}{\rho_{nf}} \tag{5}$$

where $(\rho C)_{bf}$ and $(\rho C)_p$ are the heat capacities of the base fluid and the nanoparticles, respectively.

Property	Basic fluid (water)	Nanoparticles (CuO)
Specific heat ($J\,kg^{-1}\,K^{-1}$)	4,179	535.6
Density ($kg\,m^{-3}$)	997.1	6,350
Thermal conductivity ($W\,m^{-1}\,K^{-1}$)	0.605	69
Viscosity (Pa s)	8.91×10^{-4}	–

Sources: Ho *et al.* (2008) and Heris *et al.* (2011)

Table I. Thermophysical properties of base fluid and nanoparticles at 293 K

The effective thermal conductivity k_{nf} of the nanofluid (Yu and Choi, 2003) is:

$$k_{nf} = \frac{k_p + 2k_{bf} + 2(k_p - k_{bf})(1+\gamma)^3\phi}{k_p + 2k_{bf} - 2(k_p - k_{bf})(1+\gamma)^3\phi} k_{bf} \tag{6}$$

where k_{bf} and k_P are the thermal diffusivities of the base fluid and the nanoparticles, respectively. Additionally, γ is the ratio of the nano-layer thickness to the original particle radius, which is considered to be 0.1.

The effective viscosity μ_{nf} of the nanofluid (Gosselin and da Silva, 2004; Rostamani *et al.*, 2010) is:

$$\mu_{nf} = \frac{\mu_{bf}}{(1-\phi)^{2.5}} \tag{7}$$

where μ_{bf} is the dynamic viscosity of the base fluid.

Water-based CuO nanofluids with various volume fractions (0.1, 0.2, 0.5, and 0.8 percent) are used as working fluids. In addition, for comparison, water is also employed as the working fluid. Variations of the transport properties with nanoparticle volume fraction are shown in Table II. The convective heat transfer coefficient is investigated for various Reynolds numbers in the range of $4{,}000 < Re < 10{,}000$. Re_{nf}, Pr_{nf}, and Pe_{nf} are the Reynolds, Prandtl, and Peclet numbers of the nanofluid, respectively, expressed as:

$$\mathrm{Re}_{nf} = \frac{\rho_{nf}\overline{U}D_h}{\mu_{nf}} \tag{8}$$

$$\mathrm{Pr}_{nf} = \frac{C_{nf}\mu_{nf}}{k_{nf}} \tag{9}$$

$$Pe_{nf} = \mathrm{Re}_{nf}\mathrm{Pr}_{nf} = \frac{\rho_{nf}C_{nf}\overline{U}D_h}{k_{nf}} \tag{10}$$

2.3 Turbulence modeling

In the present numerical study, the $\kappa - \varepsilon$ turbulent model proposed by Launder and Spalding (1972) is adopted. The $\kappa - \varepsilon$ turbulent model introduces two additional equations, namely those for turbulent kinetic energy (κ) and rate of dissipation (ε), given, respectively, as:

$$div(\rho\overline{V}\kappa) = div\{(\mu + \mu_t)/\sigma_\kappa \nabla\kappa\} + G_\kappa - \rho\varepsilon \tag{11}$$

$$div(\rho\overline{V}\varepsilon) = div\{(\mu + (\mu_t/\sigma_\varepsilon)\nabla\varepsilon\} + C_{1\varepsilon}(\varepsilon/\kappa)G_\kappa + C_{2\varepsilon}\rho(\varepsilon^2/\kappa) \tag{12}$$

Table II. Variations of the transport properties with nanoparticle volume fraction

Property	Particle volume concentration 0.0%	0.1%	0.2%	0.6%	0.8%
Density (kg m^{-3})	997.1	1,002.45	1,007.81	1,029.22	1,039.92
Specific heat (J kg^{-1} K^{-1})	4,179	4,155.92	4,133.09	4,044.13	4,001.02
Thermal conductivity (W m^{-1} K^{-1})	0.605	0.6081	0.6113	0.6241	0.6306
Viscosity (Pa s)	8.91×10^{-4}	8.93×10^{-4}	8.95×10^{-4}	9.05×10^{-4}	9.09×10^{-4}

where G_κ represents the generation of turbulent kinetic energy due to mean velocity gradients; σ_κ and σ_ε are effective Prandtl numbers for turbulent kinetic energy and rate of dissipation, respectively; $C_{1\varepsilon}$ and $C_{2\varepsilon}$ are constants; μ_t is the eddy viscosity, modeled as:

$$\mu_t = \left(\rho C_\mu \kappa^2\right)/\varepsilon \tag{13}$$

where C_μ is a constant whose value is 0.09.

In Equations (11) and (12): $C_{1\varepsilon} = 1.44$, $C_{2\varepsilon} = 1.92$, $\sigma_\kappa = 1.0$, and $\sigma_\varepsilon = 1.3$.

Further information regarding turbulence modeling is available in a study by Launder and Spalding (1972) and the Fluent Inc. (2012).

2.4 Boundary conditions

The governing equations of the fluid flow are nonlinear coupled partial differential equations. Boundary conditions are specified as follows. At the duct inlet section, uniform axial velocity $\overline{U}$, temperature T_{in}, turbulent intensity, and hydraulic diameter (Fluent Inc., 2012) are specified. At the outlet section, the flow and temperature field are assumed to be fully developed. The outflow boundary condition is implemented for the outlet section, that is, zero normal gradients prevail for all flow variables except pressure. On the tube wall, the no-slip and constant heat flux boundary conditions are applied. In the present analysis, the near wall treatment was based on enhanced wall function (Fluent Inc., 2012).

2.5 Solver

ANSYS FLUENT computational fluid dynamics (CFD) software incorporated with the finite volume method is employed to solve the nonlinear governing equations (Equations (1)-(3), (11), and (12)) of turbulent forced convection heat transfer in a square cross-section duct with a constant heat flux. The control-volume-based technique is used to convert a general scalar transport equation into an algebraic equation that can be solved numerically. It consists of: division of the domain into discrete control volumes using a computational grid; integration of the governing equations on the individual control volumes to construct algebraic equations for the discrete dependent variables (unknowns) such as velocities, pressure, and temperature; and linearization of the discretized equations and solution of the resultant linear equation system to yield updated values of the dependent variables (ANSYS Inc., 2009). Details about the solver algorithms used by ANSYS FLUENT can be found in the ANSYS Inc. (2009).

Figure 1 illustrates the geometrical configuration used in the simulation. A 1.0-m-long duct with a square cross-sectional area of 1 cm^2 is employed, which is exactly the same as that used in Mehrjou *et al.*'s (2015) experiment. The Geometry and Mesh Building Intelligent Tool model (ANSYS Inc., 2009) is adopted to describe the problem. The model graphs and meshes the spatial domain with 200 × 50 × 50 grids (duct length of 200 and a square cross-sectional area of 50 × 50).

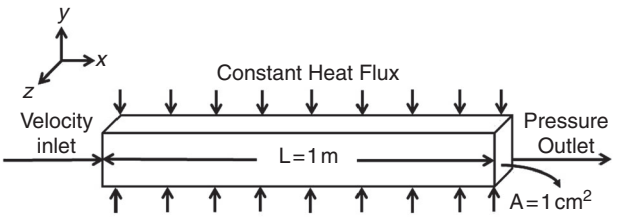

Figure 1. Geometrical configuration used in simulation

The numerical simulation is carried out at various Peclet numbers and particle concentrations (0.1, 0.2, 0.5, and 0.8 vol%). The particle diameter is 40 nm. The finite volume formulation is used with the semi-implicit method for pressure-linked equations algorithm to solve the discretized equations derived from the partial nonlinear differential equations of the mathematical model. The convection terms of the transport equations are discretized by the second-order hybrid central differences/upwind scheme. During the calculation, the residuals of the algebraic discretized equations, resulting from the spatial integration of the conservation equations over finite control volumes, are monitored. Simulations are considered to be converged when the residuals for all discretized equations are smaller than 10^{-6}. Then, the heat transfer coefficient and Nusselt number are, respectively, calculated using the following equations:

$$\overline{h_{nf}} = \frac{C_{nf}\rho_{nf}\overline{U}A\left(T_{b,o}-T_{b,i}\right)}{\pi D_h L(T_w-T_b)_M} \tag{14}$$

$$\overline{Nu_{nf}} = \frac{\overline{h_{nf}}D_h}{k_{nf}} \tag{15}$$

where $\overline{h_{nf}}$ and $\overline{Nu_{nf}}$ are the average heat transfer coefficient and Nusselt number of the nanofluid, respectively; L is the length of the duct; D_h is the hydraulic diameter of the duct; $\overline{U}$ is the mean velocity of the nanofluid at the inlet; $(T_w-T_b)_M$ is the mean temperature difference; $T_{b,i}$ and $T_{b,o}$ are the inlet and outlet bulk temperature of the nanofluid, respectively.

3. Results and discussion

3.1 Grid independence analysis and validation

Initially, to carry out the grid independence analysis, several non-uniform grids were subjected to an extensive testing procedure. For this purpose, grid densities of $200 \times 30 \times 30$, $200 \times 40 \times 40$, and $200 \times 50 \times 50$ were tested and the results were compared. Moreover, to validate the accuracy and reliability of the present CFD analysis, the calculated results are compared with the experimental data (Mehrjou *et al.*, 2015) and theoretical solutions calculated using Equation (16), i.e., Dittus-Boelter equation (Incropera and DeWitt, 2011), for the Nusselt number vs the Peclet number:

$$Nu = 0.023\mathrm{Re}^{0.8}\mathrm{Pr}^{0.4} \tag{16}$$

Figure 2 shows the effects of the number of mesh points on the Nusselt number when distilled water (base fluid) is employed as the working fluid. Figure 2 also demonstrates a comparison among the calculated, experimental (Mehrjou *et al.*, 2015), and theoretical (Incropera and DeWitt, 2011) results in the fully developed turbulent regime. The results of the present CFD analysis with grid densities of $200 \times 50 \times 50$ show good agreement with those of experimental (Mehrjou *et al.*, 2015) and theoretical (Incropera and DeWitt, 2011) studies. Therefore, in this study, the numbers of grid points in the x-, y-, and z-directions are set to 200, 50, and 50, respectively, in the following calculations.

In order to demonstrate the validity and precision of the model as well as numerical procedure, the friction factor is also calculated and compared with the Darcy friction correlation given by Blasius (White, 1991):

$$f = 4C_f = 4\left(0.0791\mathrm{Re}^{-1/4}\right) \tag{17}$$

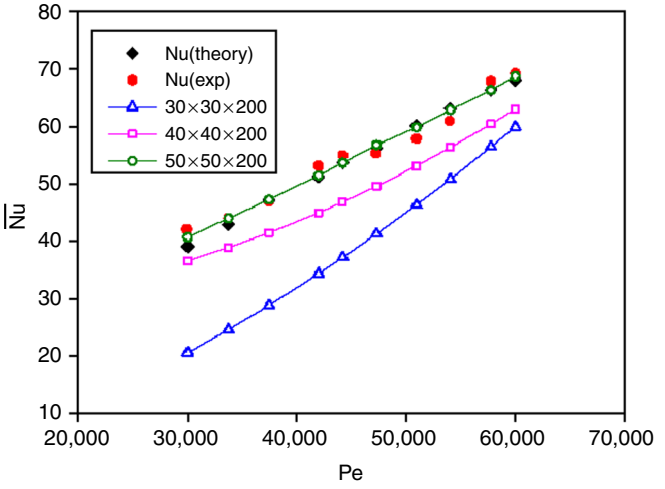

Figure 2.
Grid sensitivity testing and comparison among numerical, theoretical, and experimental data for Nusselt number of water

As shown in Figure 3, good agreements between the present computed predictions (with grid densities of $200 \times 50 \times 50$) and the theoretical results (White, 1991) are observed over the range of the Reynolds number studied.

3.2 Effects of Peclet number, Reynold number, and particle volume concentration

Figure 4 shows a comparison between numerical and experimental data for the heat transfer coefficient vs the Peclet number at various particle volume concentrations for CuO-water nanofluids. It is found that increasing the particle volume concentration results in a significant increase in the heat transfer coefficient. This is due to an increase in fluid thermal conductivity and an increase of energy exchange rate resulting from the irregular and chaotic motion of ultra-fine particles in the fluid (Xuan and Li, 2000). Additionally, the Peclet number (or Reynolds number) significantly affects heat transfer characteristics. A higher Peclet number (or Reynolds number) corresponds to higher fluid velocity and

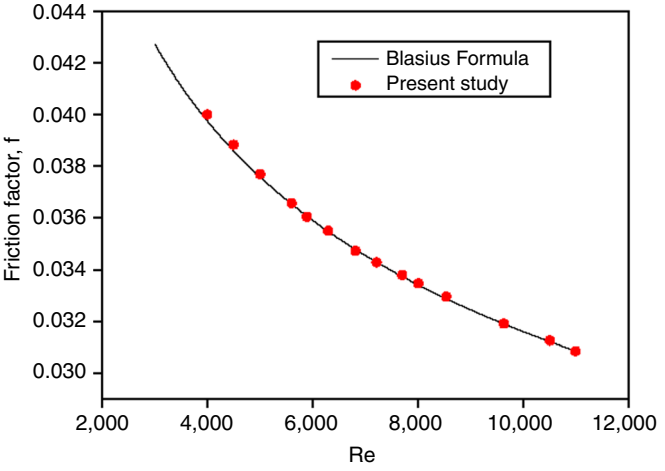

Figure 3.
Comparison of Darcy friction factor and Blasius formula with computed values for water in turbulent regime

temperature gradient, which in turn results in a higher value of the heat transfer coefficient. With a constant nanoparticle volume fraction, the increment of Pe (or Re) with the nanofluid flow rate leads to convective heat transfer enhancement. This heat transfer enhancement may be caused by more chaotic movement and nanoparticle migration, especially near the duct corner through the flow (Heris *et al.*, 2013; Mehrjou *et al.*, 2015). It is worth noting that at a particle volume concentration of 0.8 percent, the enhancement of the convective heat transfer coefficient of CuO-water nanofluid (19.63 percent) is much higher than that of the effective thermal conductivity (3.15 percent). Accordingly, the enhancement of the convective heat transfer cannot be solely attributed to the enhancement of the effective thermal conductivity. Other factors such as dispersion (Wen and Ding, 2005), Brownian motion (Heyhat and Kowsary, 2010), thermophoresis (Heyhat and Kowsary, 2010), and nanoparticle migration (Wen and Ding, 2005; Heyhat and Kowsary, 2010; Bahiraei *et al.*, 2014) may also be responsible for the enhancement of convective heat transfer (Heris *et al.*, 2013).

Figure 5 shows a comparison between the simulated average nanofluid convective heat transfer coefficient $\overline{h_{nf}}(sim)$ and the experimental average nanofluid convective heat transfer coefficient $\overline{h_{nf}}(\exp)$. The results show that the simulated average nanofluid convective heat transfer coefficient coincides well with the experimental average nanofluid convective heat transfer coefficient (Mehrjou *et al.*, 2015). The discrepancies are in the range of −8 to +7.5 percent.

Figure 6 shows a comparison between numerical and experimental data for the Nusselt number vs the Reynold number at various particle volume concentrations for CuO-water nanofluids. It is obvious that the heat transfer performance of the nanofluid with respect to the enhancement of Nusselt number is significantly higher than that of distilled water. This is caused by the remarkable surface area of nanoparticles and their self-interactions, and also between the nanoparticles and the inner surface of the duct during flow through the duct (Mehrjou *et al.*, 2015). The turbulence of the nanofluid flow through the duct leads to the good dispersion of nanoparticles. Therefore, good dispersion of nanoparticles decreases the thermal boundary layer thickness. Due to the inverse proportion of the convective heat transfer coefficient to the boundary layer thickness, and the direct proportion of the Nusselt number to convective heat transfer coefficient, the heat transfer enhancement is increased considerably for nanofluids.

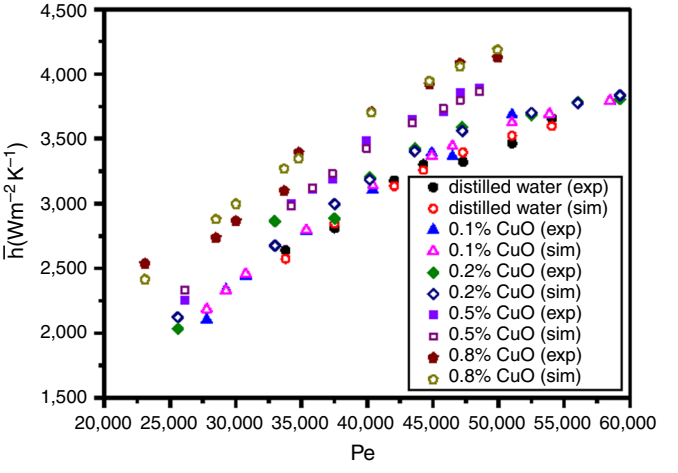

Figure 4.
Comparison between numerical and experimental data for heat transfer coefficient vs Peclet number at various particle volume concentrations for CuO-water nanofluids

Figure 7 shows a comparison between the simulated average Nusselt numbers $\overline{Nu}(sim)$ and the experimental average Nusselt numbers $\overline{Nu}(exp)$. The results show that the simulated average Nusselt numbers coincide well with the experimental average Nusselt numbers. The discrepancies are in the range of −9 to +9.5 percent.

Figure 8 shows a comparison of the average heat transfer coefficient between the present CFD results and the experimental ones (Mehrjou *et al.*, 2015). It is clear that the results of the average heat transfer coefficient obtained from the numerical simulation coincide well with published experimental data (Mehrjou *et al.*, 2015). It is also found that the heat transfer coefficient increases with the particle volume concentration and Peclet number.

Figure 9 shows a comparison between $\overline{h_{nf}}(sim)/\overline{h_{nf}}(th)$ and $\overline{h_{nf}}(exp)/\overline{h_{nf}}(th)$, where $\overline{h_{nf}}(exp)$ and $\overline{h_{nf}}(sim)$ are experimental (Mehrjou *et al.*, 2015) and simulated

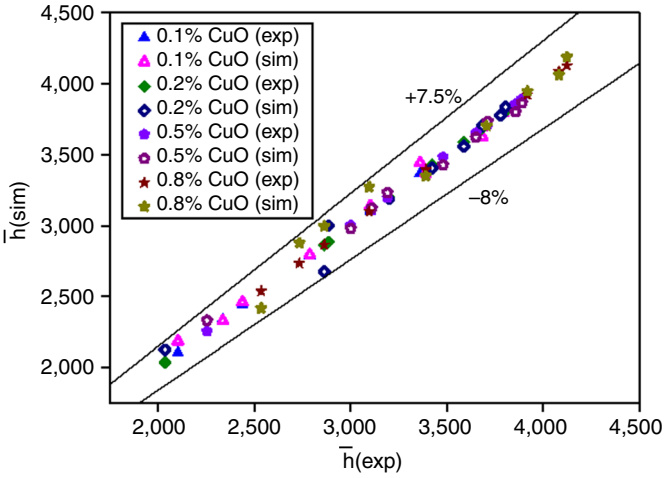

Figure 5.
Comparison between numerical heat transfer coefficient and experimentally measured heat transfer coefficient at various particle volume concentrations for CuO-water nanofluids

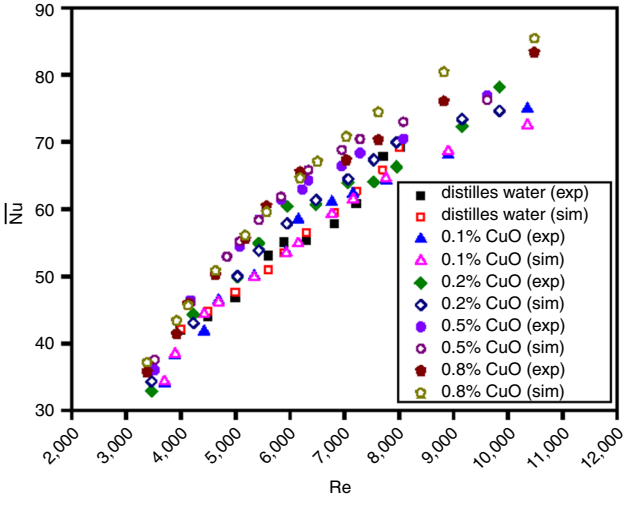

Figure 6.
Comparison between numerical and experimental data for Nusselt number vs Reynold number at various particle volume concentrations for CuO-water nanofluids

average heat transfer coefficients, respectively; $\overline{h_{nf}}(th)$ is the theoretical convective heat transfer coefficient calculated from the Dittus-Boelter equation (Incropera and DeWitt, 2011). $\overline{h_{nf}}(sim)/\overline{h_{nf}}(th)$ denotes the ratio of the simulated average heat transfer coefficient to the theoretical one calculated from the Dittus-Boelter equation, and $\overline{h_{nf}}(exp)/\overline{h_{nf}}(th)$ designates the ratio of the experimental average heat transfer coefficient to the theoretical one calculated from the Dittus-Boelter equation. As can be observed, the ratio of the simulated average heat transfer coefficient to the theoretical one is in good agreement with that of the experimental average heat transfer coefficient to the theoretical one. The discrepancies are in the range of -4 to $+5$ percent.

Table III illustrates the differences between wall and bulk temperatures at various nanoparticle concentrations at the inlet and outlet of the studied square duct. According to these data, for a constant wall heat flux boundary condition, the

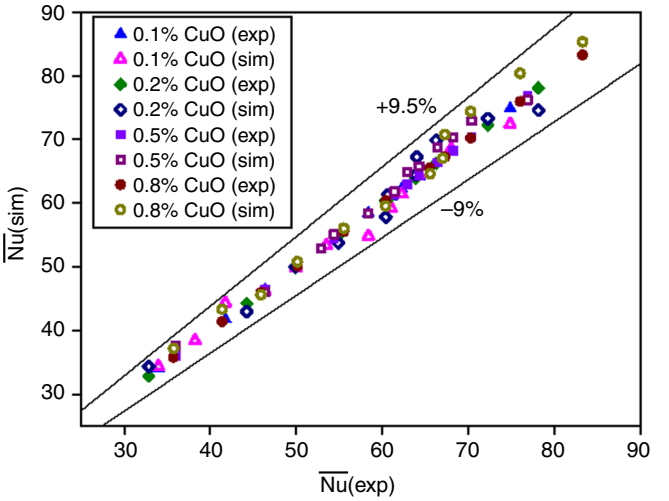

Figure 7.
Comparison between numerical Nusselt number and experimentally measured Nusselt number at various particle volume concentrations for CuO-water nanofluids

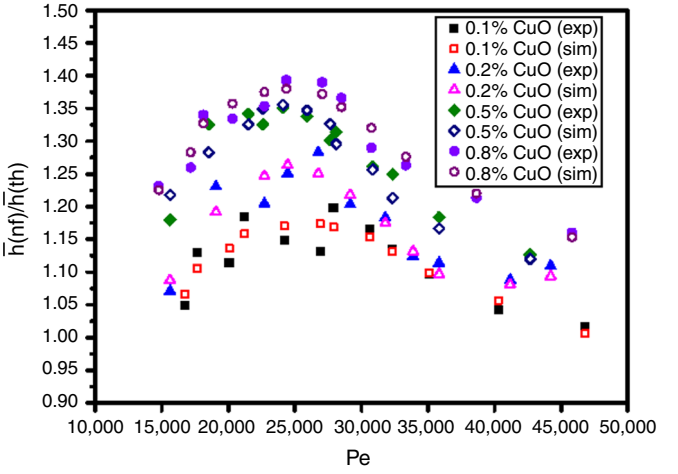

Figure 8.
Comparison between numerical and experimental convective heat transfer coefficient to Dittus-Boelter equation vs Peclet number at various particle volume concentrations for CuO-water nanofluids

differences between the wall and bulk temperatures decrease with increasing particle volume concentration of the nanofluid. Clearly, the rate of decrease in the temperature difference for the outlet section is significant, which shows the capability of nanofluids to remove the heat at the wall effectively in square ducts.

4. Conclusion

Turbulent flow forced convection of CuO-water nanofluid in a square cross-section duct subjected to a constant heat flux was numerically studied. The results show that the heat transfer coefficient and Nusselt number increase with increasing Peclet number and particle volume concentration. The heat transfer coefficient of CuO-water nanofluids increased by 19.63 percent at a particle concentration of 0.8 vol% compared with that of pure water at Pe = 49,000. It is worth noting that at this particle volume concentration (0.8 percent), the enhancement of the convective heat transfer coefficient of the CuO-water nanofluid (19.63 percent) is much higher than that of the effective thermal conductivity (3.15 percent). Hence, the enhancement of the convective heat transfer cannot be solely attributed to the enhancement of the effective thermal conductivity. Other factors such as dispersion, Brownian motion, thermophoresis, and nanoparticle migration may also be responsible for the enhancement of convective heat transfer. Additionally, theoretical correlations calculated from the Dittus-Boelter equation (proposed for the turbulent flow of a single-phase fluid) are not able to predict

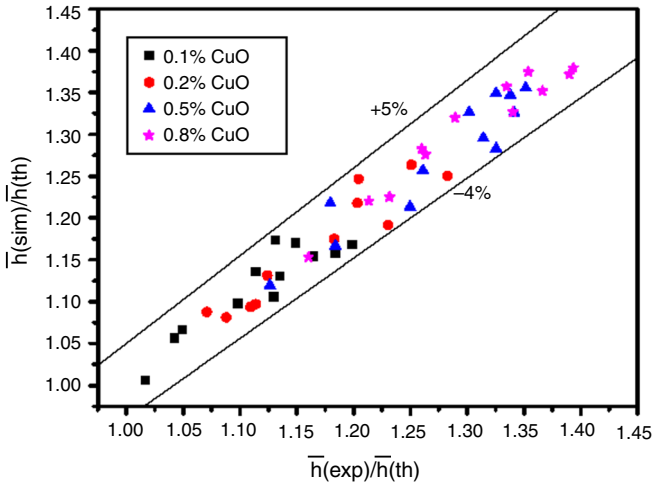

Figure 9. Comparison between numerical and experimental convective heat transfer coefficient to Dittus-Boelter equation at various particle volume concentrations for CuO-water nanofluids

Volume concentration	0% (base fluid)	0.1%	0.2%	0.8%
Experimental				
$(T_w - T_b)$ for inlet section	7.9	6.9	6.3	6.2
$(T_w - T_b)$ for outlet section	4.4	3.4	3.1	2.6
Simulation				
$(T_w - T_b)$ for inlet section	7.5259	6.6164	6.1092	6.1681
$(T_w - T_b)$ for outlet section	4.5046	3.5331	3.2732	3.0120

Table III. Differences between wall and bulk temperatures for various particle concentrations of nanofluids at inlet and outlet of duct

nanofluid thermal performance. Moreover, the differences between the wall and bulk temperatures decrease with increasing volume concentration of nanoparticles. Finally, the present numerical results are in good agreement with the published experimental data.

References

Ahmed, H.E., Ahmed, M.I., Yusoff, M.Z., Hawlader, M.N.A. and Al-Ani, H. (2015), "Experimental study of heat transfer augmentation in non-circular duct using combined nanofluids and vortex generator", *International Journal of Heat and Mass Transfer*, Vol. 90, pp. 1197-1206.

Akbar, N.S., Raza, M. and Ellahi, R. (2014), "Influence of heat generation and heat flux on peristaltic flow with interacting nanoparticles", *European Physical Journal – Plus*, Vol. 129 No. 8, pp. 1-15.

ANSYS Inc. (2009), *ANSYS FLUENT Workbench User's Guide; Release 12.1*, ANSYS, Cecil Township, PA.

Bahiraei, M., Mostafa Hosseinalipour, S. and Hangi, M. (2014), "Prediction of convective heat transfer of Al_2O_3-water nanofluid considering particle migration using neural network", *Engineering Computations*, Vol. 31 No. 5, pp. 843-863.

Bianco, V., Manca, O. and Nardini, S. (2013), "Second law analysis of Al_2O_3-water nanofluid turbulent forced convection in a circular cross section tube with constant wall temperature", *Advances in Mechanical Engineering*, Vol. 2013, pp. 1-12.

Bianco, V., Manca, O. and Nardini, S. (2014), "Performance analysis of turbulent convection heat transfer of Al_2O_3 water-nanofluid in circular tubes at constant wall temperature", *Energy*, Vol. 77, pp. 403-413.

Buongiorno, J. (2006), "Convective transport in nanofluids", *Journal of Heat Transfer – Transactions of the Asme*, Vol. 28 No. 3, pp. 240-250.

Corcione, M. (2010), "Heat transfer features of buoyancy-driven nanofluids inside rectangular enclosures differentially heated at the sidewalls", *International Journal of Thermal Science*, Vol. 49 No. 9, pp. 1536-1546.

Eastman, J.A., Choi, S.U.S., Soyez, S., Li, G., Thompson, L.J. and DiMelfi, R.J. (1999), "Novel thermal properties of nanostructured materials", *Journal of Metastable and Nanocrystalline Materials*, Vols 2-6, pp. 629-634.

Ellahi, R., Hassan, M. and Zeeshan, A. (2015), "Shape effects of nanosize particles in Cu-H_2O nanofluid on entropy generation", *International Journal of Heat and Mass Transfer*, Vol. 81, pp. 449-456.

Etemad, S.Gh., Farajollahi, B., Hajipour, M. and Thibault, J. (2012), "Turbulent convective heat transfer of suspensions of γ-Al_2O_3 and CuO nanoparticles (nanofluids)", *Journal of Enhanced Heat Transfer*, Vol. 19 No. 3, pp. 191-197.

Fluent Inc. (2012), *Fluent 14.5 User Guide*, ANSYS, Canonsburg, PA.

Gosselin, L. and da Silva, A. (2004), "Combined heat transfer and power dissipation optimization of nanofluid flow", *Applied Physics Letters*, Vol. 85 No. 18, pp. 4160-4162.

Heris, S.Z., Nassan, T.H. and Noie, S.H. (2011), "CuO/water nanofluid convective heat transfer through square duct under uniform heat flux", *International Journal of Nanoscience and Nanotechnology*, Vol. 7 No. 3, pp. 111-120.

Heris, S.Z., Nassan, T.H., Noie, S.H., Sardarabadi, H. and Sardarabadi, M. (2013), "Laminar convective heat transfer of Al_2O_3/water nanofluid through square cross-sectional duct", *International Journal of Heat and Fluid Flow*, Vol. 44, pp. 375-382.

Heyhat, M.M. and Kowsary, F. (2010), "Effect of particle migration on flow and convective heat transfer of nanofluids flowing through a circular pipe", *Journal of Heat Transfer – Transactions of the ASME*, Vol. 132 No. 6, pp. 1-9.

Ho, C.J., Chen, M.W. and Li, Z.W. (2008), "Numerical simulation of natural convection of nanofluid in a square enclosure: effect due to uncertainties of viscosity and thermal conductivity", *International Journal of Heat and Mass Transfer*, Vol. 51 No. 17, pp. 4506-4516.

Incropera, F.P. and DeWitt, D.P. (2011), *Introduction to Heat Transfer*, 4th ed., John Wiley & Sons, New York, NY, p. 179.

Kakaç, S. and Pramuanjaroenkij, A. (2009), "Review of convective heat transfer enhancement with nanofluids", *International Journal of Heat and Mass Transfer*, Vol. 52 No. 13, pp. 3187-3196.

Koo, J. and Kleinstreuer, C. (2005), "Laminar nanofluid flow in microheat-sinks", *International Journal of Heat and Mass Transfer*, Vol. 48 No. 13, pp. 2652-2661.

Launder, B.E. and Spalding, D.B. (1972), *Mathmatical Models of Turbulence*, Academic Press, New York, NY.

Mehrjou, B., Heris, S.Z. and Mohamadifard, K. (2015), "Experimental study of CuO/water nanofluid turbulent convective heat transfer in square cross-section duct", *Experimental Heat Transfer*, Vol. 28 No. 3, pp. 282-297.

Mirmasoumi, S. and Behzadmehr, A. (2008), "Numerical study of laminar mixed convection of a nanofluid in a horizontal tube using two-phase mixture model", *Applied Thermal Engineering*, Vol. 28 No. 7, pp. 717-727.

Mohammed, H.A., Bhaskaran, G., Shualib, N.H. and Abu-Mulaweh, H.I. (2011a), "Influence of nanofluids on parallel flow square microchannel heat exchanger performance", *International Communications in Heat and Mass Transfer*, Vol. 38 No. 1, pp. 1-9.

Mohammed, H.A., Bhaskaran, G., Shualib, N.H. and Saidur, R. (2011b), "Numerical study of heat transfer enhancement of counter flow of nanofluids in rectangular microchannel heat exchanger", *Superlattice Microst*, Vol. 50 No. 3, pp. 215-233.

Mwesigye, A. and Huan, Z. (2015), "Thermodynamic analysis and optimization of fully developed turbulent forced convection in a circular tube with water-Al_2O_3 nanofluid", *International Journal of Heat and Mass Transfer*, Vol. 89, pp. 694-706.

Rostamani, M., Hosseinizadeh, S.F., Gorji, M. and Khodadadi, J.M. (2010), "Numerical study of turbulent forced convection flow of nanofluids in a long horizontal duct considering variable properties", *International Communications in Heat and Mass Transfer*, Vol. 37 No. 10, pp. 1426-1431.

Santra, A.K., Sen, S. and Chakraborty, N. (2009), "Study of heat transfer due to laminar flow of copper-water nanofluid through two isothermally heated parallel heat plates", *International Journal of Thermal Sciences*, Vol. 48 No. 2, pp. 391-400.

Shahi, M., Mahmoudi, A.H. and Talebi, F. (2010), "Numerical study of mixed convective cooling in a square cavity ventilated and partially heated from the below utilizing nanofluid", *International Communications in Heat and Mass Transfer*, Vol. 37 No. 2, pp. 201-213.

Sheikholeslami, M., Bandpy, M.G., Ellahi, R. and Zeeshan, A. (2014a), "Simulation of MHD CuO-water nanofluid flow and convective heat transfer considering Lorentz forces", *Journal of Magnetism and Magnetic Materials*, Vol. 369, pp. 69-80.

Sheikholeslami, M., Ellahi, R., Hassan, M. and Soleimani, S. (2014b), "A study of natural convection heat transfer in a nanofluid filled enclosure with elliptic inner cylinder", *International Journal of Numerical Methods for Heat and Fluid Flow*, Vol. 24 No. 8, pp. 1906-1927.

Ting, H.H. and Hou, S.S. (2015), "Investigation of laminar convective heat transfer for Al_2O_3-water nanofluids flowing through a square cross-section duct with a constant heat flux", *Materials*, Vol. 8 No. 8, pp. 5321-5335.

Wen, D. and Ding, Y. (2005), "Effect of particle migration on heat transfer in suspensions of nanoparticles flowing through minichannels", *Microfluidics and Nanofluidics*, Vol. 1 No. 2, pp. 183-189.

White, F.M. (1991), *Viscous Fluid Flow*, 2nd ed., McGraw Hill, New York, NY.

Xuan, Y. and Li, Q. (2000), "Heat transfer enhancement of nanofluids", *International Journal of Heat and Fluid Flow*, Vol. 21 No. 1, pp. 58-64.

Xuan, Y. and Li, Q. (2003), "Investigation on convective heat transfer and flow features of nanofluids", *Journal of Heat Transfer*, Vol. 125 No. 1, pp. 151-155.

Yu, W. and Choi, S.U.S. (2003), "The role of interfacial layers in the enhanced thermal of nanofluids: a renovated Maxwell model", *Journal of Nanoparticle Research*, Vol. 5 Nos 1-2, pp. 167-171.

Yue, L., Lu, X., Chi, H., Guo, Y., Xu, L., Fang, W., Li, Y. and Hu, S. (2014), "Heat-sink enhancement of decalin and aviation kerosene prepared as nanofluids with palladium nanoparticles", *Fuel*, Vol. 121, pp. 149-156.

Corresponding author
Shuhn-Shyurng Hou can be contacted at: sshou@mail.ksu.edu.tw